Spatiotemporal Heterogeneity in the Distribution of Chikungunya and Zika Virus Case Incidences and Risk Factors During Their Epidemics in Barranquilla, Colombia, between 2014 and 2016: An Ecological Study

Thomas C McHale[1,] Claudia M Romero-Vivas[2], Claudio Fronterre[1], Pedro Arango-Padilla[3], Andrew K Falconar[2], Naomi R Waterlow[1], Chad Nix[1], Jorge Cano[1]*

[1]Faculty of Infectious & Tropical Diseases, London School of Hygiene & Tropical Medicine, London, United Kingdom WCIE 7HT

[2]Departamento de Medicina, Universidad del Norte, Barranquilla, Colombia

[3]Programa de Prevención y Control de Enfermedades Trasmitidas por Vectores, Secretaria de Salud Distrital, Barranquilla, Colombia

*Correspondence: Jorge Cano, jorge.cano@lshtm.ac.uk

ABSTRACT

Chikungunya virus (CHIKV) and Zika virus (ZIKV) have recently emerged as global infections with consequential disability adjusted life years (DALYs) and economic burden. This study aimed to explore the spatiotemporal heterogeneity in the occurrence of CHIKV and ZIKV outbreaks throughout Barranquilla, Colombia during 2014 and 2016 and explored the potential for clustering. Incidence data were fitted using multiple Bayesian Poisson models based on a suite of explanatory variables as potential risk factors and multiple options for random effects. A best fit model was used to analyse the case incidence risk for both epidemics to identify any risk factors during their epidemics.

Neighbourhoods in the northern region of Barranquilla were hotspots for the outbreaks of both CHIKV and ZIKV. Additional hotspots occurred in the south-western and central regions of the CHIKV and ZIKV outbreaks, respectively. Multivariate conditional autoregressive models strongly identified higher socioeconomic strata (SES) and residing in detached houses as risk factors for ZIKV case incidences.

These novel findings challenge the belief that these infections are driven by social vulnerability and merits further study both in Barranquilla and throughout the tropical and subtropical regions of the world.

Key words: Chikungunya virus, Zika virus, spatial clustering, Bayesian Poisson models, conditional autoregressive models, socioeconomic risk factors, environmental risk factors

1

INTRODUCTION

Since 2013, the two emerging arboviruses, chikungunya virus (CHIKV) and Zika virus (ZIKV), transmitted by the same vector species (*Aedes aegypti*) as the dengue viruses (DENVs), have caused major outbreaks throughout the Americas. CHIKV is thought to have first arrived in the Caribbean region in 2013, and in 2014 it expanded to the mainland regions of Central and South America [1-3]. The first autochthonous ZIKV cases were reported in the north-eastern region of Brazil in late 2014 [4]. By February 2016, local transmission of ZIKV was reported in over 20 countries in the Americas, including a major outbreak in Colombia, for which 65,726 cases were reported by April 2016 [5]. Both of these arboviral infections can lead to significant disability adjusted life years (DALYs) in the affected populations [6-8]. CHIKV can lead to life-long debilitating symptoms, including chronic muscle and joint pains [6,8]. Since the outbreak of ZIKV in the Americas, overwhelming evidence has connected its infection during pregnancy with congenital abnormalities, such as foetal microcephaly and serious neurologic conditions in adults such as Guillain-Barre syndrome [9-11].

Numerous studies have assessed the local determinants of transmission for the DENVs, which in turn led to key discoveries that helped to guide public health and vector control programmes in their efforts to curb epidemics [12-14]. Studies have found similar transmission dynamics in CHIKV prevalence. For example, Sissoko *et al.* found that seroprevalence of CHIKV antibodies in Mayotte was mainly associated with lower socioeconomic status, lower education, and makeshift housing [15]. Perkins *et al* found that the seasonal and regional transmission patterns were similar in CHIKV compared to DENV [16]. Similarly, the spread of ZIKV through the Americas was predicted by models that accounted for the suitable environmental and socioeconomic conditions of the regions [17-19].

Barranquilla is the fourth largest city in Colombia, with a population of nearly 1.4 million individuals and a population density of 7,017 persons per square kilometre [20]. The city, divided into six (1-6) economic strata [5], is estimated to house 56% of its population in the poorest of those strata [21]. This city has been an epicentre of recent outbreaks of CHIKV and ZIKV [6,22]. A four-decade history of combatting the DENVs, has led Colombia to establish a highly functional surveillance system (SIVIGILA) for reportable DENV infections [23]. Case incidences of CHIKV and ZIKV were monitored by the same reporting system [24,25]. Previous studies have reported the strengths and limitations of this system [23,25].

2

In this study, we assessed the spatial and temporal heterogeneity in the CHIKV and ZIKV case incidences in the neighbourhoods of Barranquilla between 2014 and 2016. Socioeconomic, demographic, and environmental variables were evaluated to assess their possible contributions as risk factors that influenced the case incidences and distribution during their epidemics.

MATERIAL AND METHODS

CHIKV and ZIKV incidence data

The "Instituto Nacional de Salud" and "Secretaria de Salud" provided data on CHIKV and ZIKV infected cases that had been reported in Barranquilla during 2014-2016. The incidence rates were based on both clinical criteria (described below) and laboratory test confirmations. The clinical criteria for CHIKV and ZIKV infections have been regularly used along with confirmatory laboratory tests to evaluate the epidemiological characteristics of these viral infections in Latin America [6,7,26]. Cases were aggregated by neighbourhood due to the lack of more detailed geolocation information (Figure 1).

Figure 1. Map of the Barranquilla, Colombia study site. Neighbourhood names listed in Table S1, supplementary file.
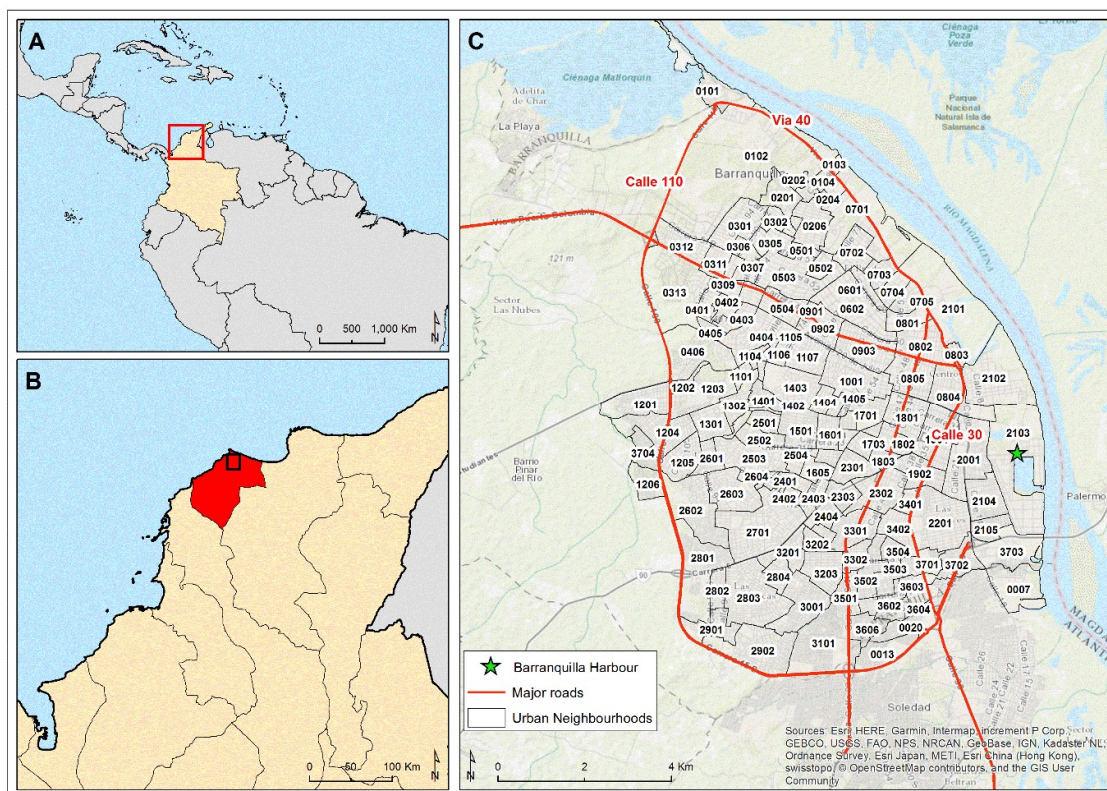
CHIKV and ZIKV infected case definitions

For the Colombian public health system, CHIKV or ZIKV infections were are identified based on clinically-assessed criteria with or without laboratory-test confirmations. The criteria for clinical confirmation of CHIKV infection included having a fever (>38ºC), sudden onset of severe arthralgia or arthritis and rash, not explained by other medical conditions, and living in a municipality where diagnosis of circulation by virological methods had previously occurred [27]. As such, laboratory confirmed CHIKV cases included viral isolation or an RT-PCR positive result for CHIKV cDNA, an anti-CHIKV IgM antibody positive result in an ELISA, or a four-fold increase in the IgG titres between paired (acute and convalescent phase) samples in the ELISA obtained within 2-14 days of each other, as described [27].

The criteria for clinical diagnosis of ZIKV infections included exanthema (rash) and fever (38ºC), and residence in a municipality with confirmed ZIKV transmission [28]. Additionally, ZIKV infection was considered when the patient had visited a high-risk area 15 days before the onset of symptoms, defined as zones below 2,200 metres above sea level in Colombia with confirmation of local ZIKV circulation, and had one or more of the following symptoms: pruritus (itchiness), arthralgia (joint pain), myalgia (muscle pain), headache, or malaise. Laboratory confirmation was achieved by obtaining a RT-PCR positive result for ZIKV cDNA, as described [11, 28].

Socioeconomic data

The total CHIKV and ZIKV infected case numbers were recorded monthly by neighbourhood for the period of 2014-2016. There were 140 neighbourhoods in Barranquilla for which population data was available during this study (Table S1).

The most recent national census for Colombia was performed in 2005, but the National Administrative Department for Statistics (DANE) had projected their populations until 2016 [20]. A Barranquilla digital map that displayed the individual neighbourhoods was obtained from the DANE website [20]. The population data and monthly incidence of CHIKV and ZIKV cases were linked within a GIS framework to this map of neighbourhoods.

The area of each neighbourhood was used to calculate the housing and population density in square kilometres for each one of them. The percent of dwellings in each neighbourhood by category (houses vs apartments) was obtained from the Barranquilla government website, as well as the percentage of males and females who resided in each neighbourhood [29].

4

In Colombia, the Central Government has defined these six socio-economic strata to classify households based on a suite of characteristics concerning the type of construction, the number of habitable rooms, water and sanitation conditions (i.e. presence of indoor toilet, existence of piped water supply, etc.) and level of urbanisation of each home's location (i.e. paved roads, availability of sewage system, etc.) [20]. This categorisation is mainly performed to differentially charge the different strata domiciliary public services thereby allowing to allocate subsidies and collect contributions in each area.

Each residence was assigned a socioeconomic stratum designation number from 1 to 6, corresponding to 1: low-low, 2: low, 3: low-medium, 4: medium, 5: medium-high, and 6: high.

Environmental data

Landsat 8 images of Barranquilla for the year 2014 (Figure S1) and 2015 (Figure S2) were obtained from United States Geological Survey website [30]. To increase the spatial resolution of multispectral bands (provided at 30m resolution) a pan-sharpening process was applied, excluding thermal infrared bands, using the 15m panchromatic band. Atmospheric correction was then conducted for bands one to eight using the DOS model-based algorithm and assuming 1% minimum reflectance [31]. Radiance and ground reflectance were subsequently obtained for each band [32]. Band combinations for ideal enhancement of vegetation were obtained from openweathermap.org [33]. A traditional infrared colour map with the band combinations of 5-4-3 was used to highlight areas of vegetation. A modification of normalised difference water index (MNDWI) image was then created to highlight areas of water [34]. These raster images were combined to define areas of vegetation, building and water coverage. Finally, zonal histogram statistics were extracted from the raster to calculate the percentage surface area of each neighbourhood that was occupied by vegetation, buildings or water. Next, the MNDWI image was used to calculate the average distance of each neighbourhood from large bodies of water identified in the raster. The Euclidian (straight-line) distance tool in ArcGIS was used to calculate the straight-line distance from the centroid of each neighbourhood to any given large body of water identified in the MNDWI. All geographical processing was performed in ArcGIS 10.3 (ESRI Inc., Redlands CA, USA) [35].

A map layer in shapefile format that identified parks and forests throughout the city was downloaded from the bbike.org website [36]. We used a high-resolution satellite map from

the city to verify the accuracy of the delineated green areas. The Euclidian distance of these identified parks or forests throughout the city were then calculated using the same approach employed to estimate distance of the residents' dwellings from water bodies. Each of the covariates listed above were then linked to the map of neighbourhoods in Barranquilla along with the monthly incidence of CHIKV and ZIKV cases.

Statistical analysis

CHIKV & ZIKV Incidence Rate

The total incidence of surveillance-defined or laboratory-confirmed CHIKV and ZIKV cases over the study period were linked to the neighbourhood shapefile. The number of recorded cases of each of these viral infections was divided by the population of each neighbourhood and multiplied by 10,000 to achieve an incidence rate of cases per neighbourhood per 10,000 persons at risk. The incidence was calculated for CHIKV and ZIKV for each individual monthly. The spatial structure of CHIKV and ZIKV case incidences over the study period of 2014 to 2016 was mapped using ArcGIS 10.3. (ESRI Inc., Redlands CA, USA) [35].

Analysis of Spatial Clustering

Exploratory analysis of spatial clustering was conducted using a global Moran's I statistic and local indicators of spatial association (LISA). The univariate Moran's I statistic was used to explore the existence of overall spatial autocorrelation for the total incidence of CHIKV and ZIKV cases throughout Barranquilla, whereas LISA analysis was implemented to explore local spatial autocorrelation and identify hotspots among neighbourhoods. An area of high-high correlation (hotspot) indicated that the estimated incidence exceeded the neighbourhood average. More details about the implementation of these statistics are provided in supplementary file (Text S1).

Differential Moran's I statistic and LISA analyses were used to explore the variation of spatial autocorrelation over time. In these differential analyses, a hotspot indicated that a higher than average case incidence in the highlighted neighbourhood during the first time period led to a higher than average case incidence in the bordering neighbourhoods during the following time period. These analyses were performed for the CHIKV and ZIKV cases for each month of their epidemics: July 2014 to April 2015 for CHIKV and October 2015 to June 2016 for ZIKV cases. GeoDa software was used to perform the exploratory spatial clustering analyses [37-40].

Missing-data imputation

The original dataset contained missing observations for some of the explanatory variables: socioeconomic stratum, housing density and the percentages of females, house dwellings and percentage of vegetation coverage. These missing values were therefore estimated using a Besag-York-Mollié conditional autoregressive (CAR) spatial model [41,42]. Details on the Bayesian model implementation are provided in a supplementary file (Text S2). For each variable an intercept-only model was fitted, and the missing observations were imputed using the resultant predictive posterior median.

Bayesian statistical modelling

Since the dataset was too sparse and noisy to fit a spatiotemporal model, the monthly counts of CHIKV and ZIKV infected cases were aggregated to consider only the potential spatial variation of the infection over the entire study period. A standardized incidence ratio (SIR) for each neighbourhood was calculated taking the distribution of cases and population into account, as follows:

$$SIR_i = \frac{O_i}{E_i}$$

where O_i is the observed number of cases, $E_i = rP_i$ is the expected number of cases, P_i is the population and $r = \frac{\sum_{i=1}^{n} O_i}{\sum_{i=1}^{n} P_i}$ is the overall incidence ratio.

This metric was used to estimate the risk of infected case incidence associated with residence in each neighbourhood.

SIR values across neighbourhoods were fitted using multiple Bayesian Poisson models with a range of explanatory variables as potential risk factors and different options for random effects with: i) no random effects, ii) independent random effects, and iii) spatially correlated random effects, implemented through a CAR.

All explanatory covariates were mean centred. In this way the intercept was interpretable as the average global SIR when the SES level was equal to low. The adequacy of these models was explored using standard posterior predictive checks and a final comparison, to select the model that best fit the data, was performed using the deviance information criterion (DIC) [43]. Details on the specifications of these Bayesian Poisson models are given in a supplementary file (Text S2).

RESULTS

Description of socioeconomic and environmental data

Among the 140 neighbourhoods included in the study, the median socioeconomic stratum was 3 with the 5th and 95th percentile including strata one and six, respectively. The median population density (projected for 2016) was 16.6 persons/km^2, whilst the median percentage of dwellings which were apartments was 33.7%. The median distances of the dwellings from a park was 473m and from water bodies was 2096m. The percentage of building coverage was high (median: 95.1%), while water and vegetation coverage were very low (median: 0%) to low (median: 4.88%), respectively and the median male to female ratio was 46.9 to 53.1 (Table 1). The northern area of Barranquilla houses the highest SES (Figure S8) while the south-western area has far higher percentages of detached houses (Figure S9).

For 21.3% (n = 30) of the neighbourhoods there was no data of their housing densities, nor was there data on the percentage of houses versus apartment for 13.5% (n = 19) of the neighbourhoods. For all other variables assessed in this study, data was not available for fewer than 5% of the neighbourhoods. Amongst the recorded cases in the original data set, no neighbourhood was known for 5.9% (n = 110) and 10.5% (n = 746) of the patients with CHIKV or ZIKV infections, respectively.

Table 1. Descriptive statistics of neighbourhoods (n = 140) for CHIKV and ZIKV infected cases and risk factors to be included in the regression analysis.

		Percentile		
	Median	**5%**	**95%**	**NA, % (n)**
Incidence of CHIKV per 10,000 residents	10.6	0	48.4	0.00 (0)
Incidence of ZIKV per 10,000 residents	50.3	0	157	0.00 (0)
Socioeconomic stratum	3	1	6	4.96 (7)
Population density (persons/km^2)	16.6	1.96	41.4	0.00 (0)
Housing density (dwellings/km^2)	3.50	0.776	6.44	21.3 (30)
Percent house dwellings	65.8	23.6	85.2	13.5 (19)
Percent apartment dwellings	33.7	11.0	71.2	13.5 (19)
Percent male	46.9	41.1	50.8	3.55 (5)
Percent female	53.1	49.2	58.9	3.55 (5)
Percent vegetation coverage	4.88	0.248	53.4	1.42 (2)

8

Percent building coverage	95.1	46.7	99.8	1.42 (2)
Percent water coverage	0	0	0.0792	1.42 (2)
Distance from large water bodies (metres)	2096	334	3961	0.71 (1)
Distance from parks (metres)	473	146	2047	0.71 (1)

NA: not available

Analysis of Chikungunya virus outbreaks

During the study period, there were a total of 1,865 cases of CHIKV in Barranquilla. The total incidence of CHIKV during the study period was 16.4 per 10,000 persons, and the incidence was 12.1, 3.65, and 0.596 per 10,000 persons in 2014, 2015, and 2016, respectively. There was a single distinct peak of CHIKV cases that began in the 4th quarter of 2014 and continued until the end of the 1st quarter of 2015 (Figure 2).

Figure 2. Incidence of CHIKV infected case notifications to SIVIGILA (N.B. the definitions are described in the Methods section). Each bar represents one week.
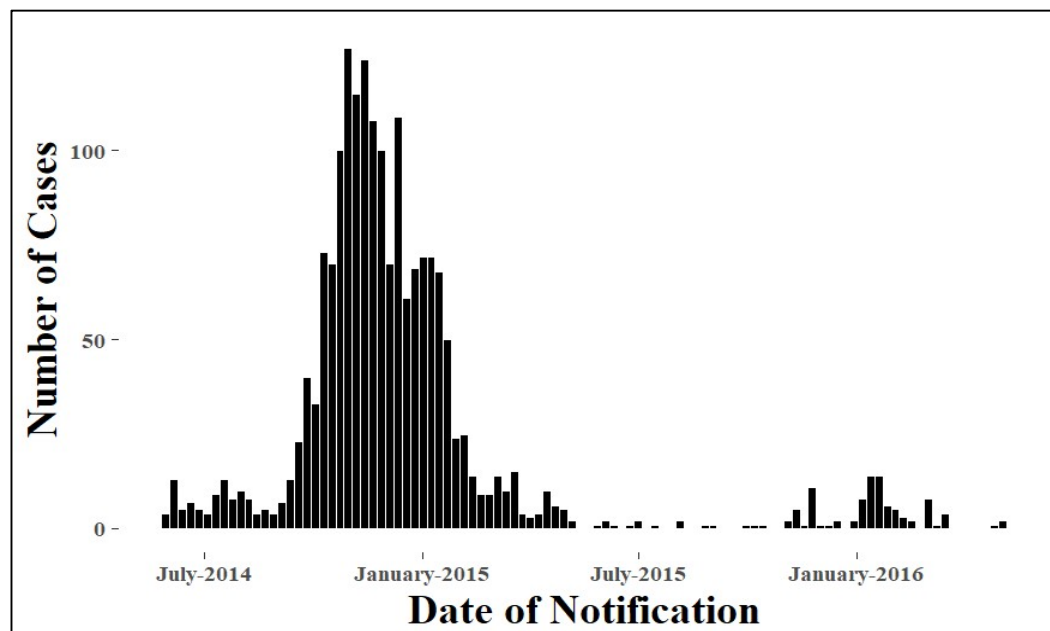

When the CHIKV incidence rate was displayed in a map by neighbourhoods, there were two clear areas of high incidence rates (within the 5th quantile), particularly in the northern (neighbourhoods: 0301, 0302, 0306, 0307 and 0308) area and the south-western (neighbourhoods: 1201, 1202, 1204, 1208, 1302, 1304, 3704) area next to the main western circular road route around the city (Figure S3 and Figure 1 for neighbourhood codes).

9

The global univariate Moran's I statistic for the total incidence of CHIKV infected cases during the study period was 0.091 (pseudo p-value 0.0026), suggesting a global clustering pattern across the study area. The LISA cluster map showed one significant cluster of high-high incidence ('hotspot') in the south-western (neighbourhoods: 1204, 1205, 1206, 2602, 3704) area of the city (Figure S4 and Figure 1 for neighbourhood codes).

The analysis of local clustering over time (differential LISA analysis) showed a clear evolution of the CHIKV epidemic, with hotspots appearing at the north-western area of the city at outbreak onset, which then moved to the south-western area. The hotspot area expanded from a single neighbourhood from August to September to four neighbourhoods in October to November, in the south-western area. Subsequently, hotspots appeared to move to the margins of the city in the northern and south-eastern regions, where the incidence rate increased sharply (Figure 3).

Figure 3. Differential monthly LISA clusters of CHIKV infected cases during the period of peak incidence (July 2014 – January 2015). Coloured neighbourhoods were significant, defined as p < 0.05. NS: not significant (grey colour).
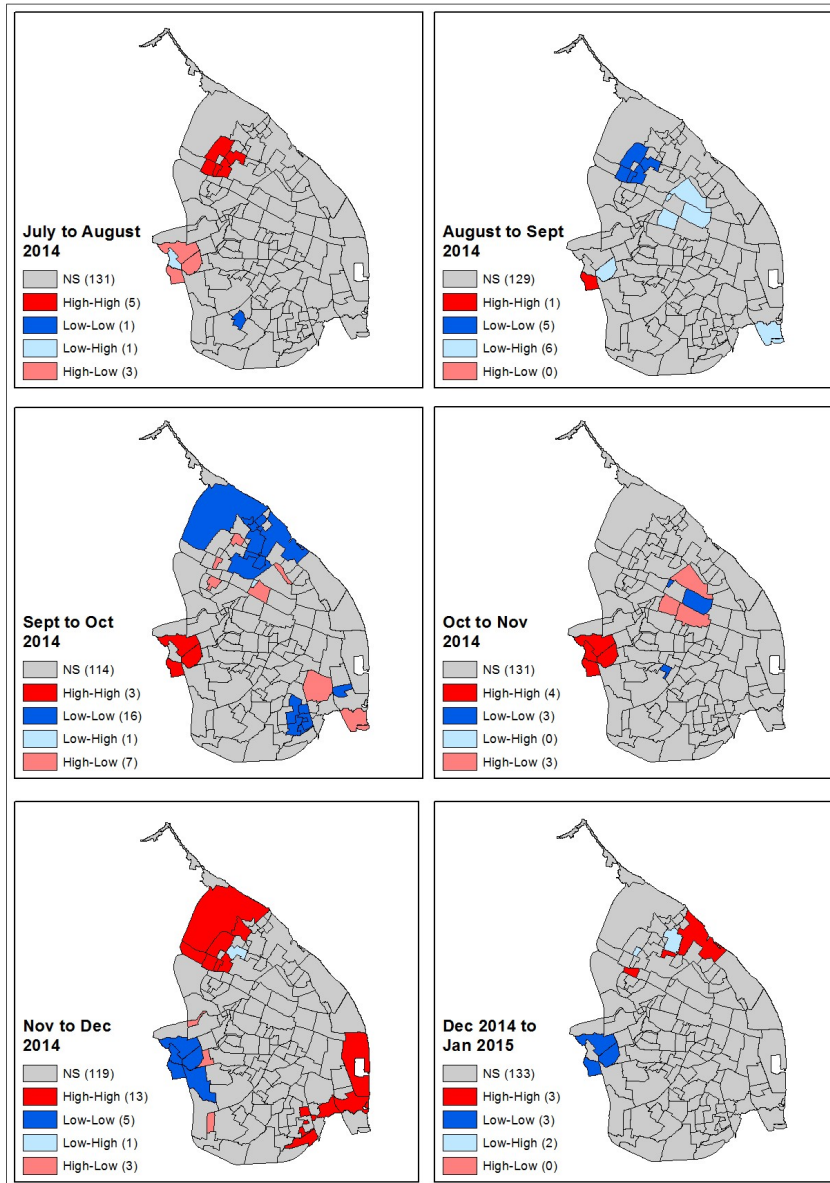
Finally, the Bayesian Poisson model of CHIKV SIR fitted with the explanatory variables (SES, population density, housing density, percentage house dwellings, female resident ratio, vegetation coverage, distance to parks and distance to water bodies) and with no random effects showed poor fitting performance of incidence data (DIC: 1217.04) (Table 4). Looking at the posterior predictive distributions and the posterior predictive p-value there were clear signs of over-dispersion: a large amount of variability in the observed SIR was not accounted

11

for by the model. We therefore introduced a set of independent random effects using the model 2 approach (Text S2) to capture the remaining variability. Since the model 1 approach showed spatial structure on the distribution of CHIKV SIR across Barranquilla, we assessed the persisting spatial correlation on the residuals for the fitted model 2, controlling for spatially varying explanatory variables. Indeed, we still observed significant global residual dependence (Moran's I statistic: 0.0716, p-value: 0.04), thus we opted to employ a set of spatially structured random effects that could cope with a global spatial correlation (model 3 approach). Model 3, globally smooth CAR model with spatially correlated random effects (Text S2), showed the better fitting performance as indicated by its DIC value (DIC: 717.03) (Table 4), and the resulting residuals no longer showed any presence of spatial dependency (Moran's I statistic: 0.0202, p-value: 0.08), thereby reinforcing our model selection. Figure 4 shows crude and fitted CHIKV SIR values throughout Barranquilla.

Figure 4. Crude SIR of CHIKV infected cases by neighbourhood during its 2014-2015 epidemic in Barranquilla. (A) Fitted globally smooth CAR model for the SIR with spatially correlated random effects and (B) the modelled SIR with spatially correlated random effects.
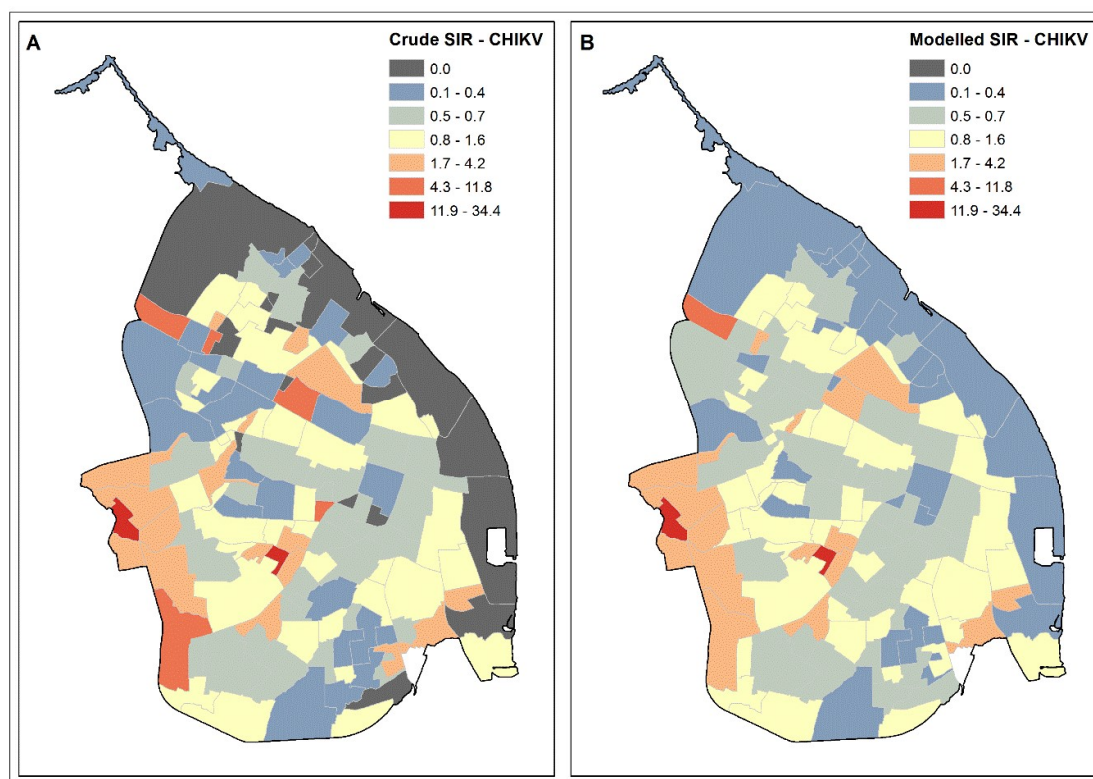
Table 2 shows the regression coefficients for the spatial fixed effects considered to fit CHIKV SIR values, based on the model 3 approach. Risk of CHIKV case incidences appeared to slightly decrease with the distance of the residents' dwellings to parks (Coefficient 0.85, 95% CI 0.44, 1.48) and water bodies (Coefficient 0.92, 95% CI 0.64, 1.33). The poorest neighbourhoods, based on three levels of SES (quantiles), were the most at risk for CHIKV infections (reference low SES, medium SES coefficient 0.42, 95% CI 0.23, 0.77; high SES 0.65, 95% CI 0.24, 1.75). The risk for CHIKV infections was increased by 11.4% for a unit percentage increase of female residents. None of these associations were, however, statistically significant.

Table 2. Posterior median and 95% credible intervals for the fixed effects of the final model for the CHIKV standardized incidence rate (SIR) during 2014-2016. These parameters are reported on the exponential scale so that the effect could be interpreted as multiplicative on the SIR. Socioeconomic strata (SES) were grouped in three categories as; high: SES 5 and 6, medium: SES 3 and 4 and low: SES 1 and 2, and regression coefficients were obtained for the medium SES and high SES compared to the low SES.

	Regression Coefficient	95% CI
Intercept	1.04	(0.68, 1.59)
Medium SES (ref. class low)	0.42	(0.23, 0.77)
High SES (ref. class low)	0.65	(0.24, 1.74)
Population density	0.99	(0.97 1.02)
Housing density	0.96	(0.86, 1.07)
Percent house dwellings	1.00	(0.99, 1.02)
Percent female	1.11	(0.99, 1.26)
Percent vegetation coverage	0.99	(0.98, 1.00)
Distance from large water bodies	0.92	(0.63, 1.33)
Distance from parks	0.85	(0.45, 1.48)

Analysis of Zika virus outbreaks

During the study period, there were a total of 7,029 ZIKV infected cases in Barranquilla. The total incidence of ZIKV was 61.7 cases per 10,000 persons at risk. The incidence of ZIKV

was 0, 12.3 and 49.4 cases per 10,000 persons during 2014, 2015 and 2016, respectively. There was a single distinct peak of ZIKV cases that began at the beginning of the 4th quarter of 2015 and continued until the end of the 1st quarter of 2016 (Figure 5).

Figure 5. Incidence of ZIKV infected case notifications to SIVIGILA (N.B. the definitions described in methods). Each bar represents one week.
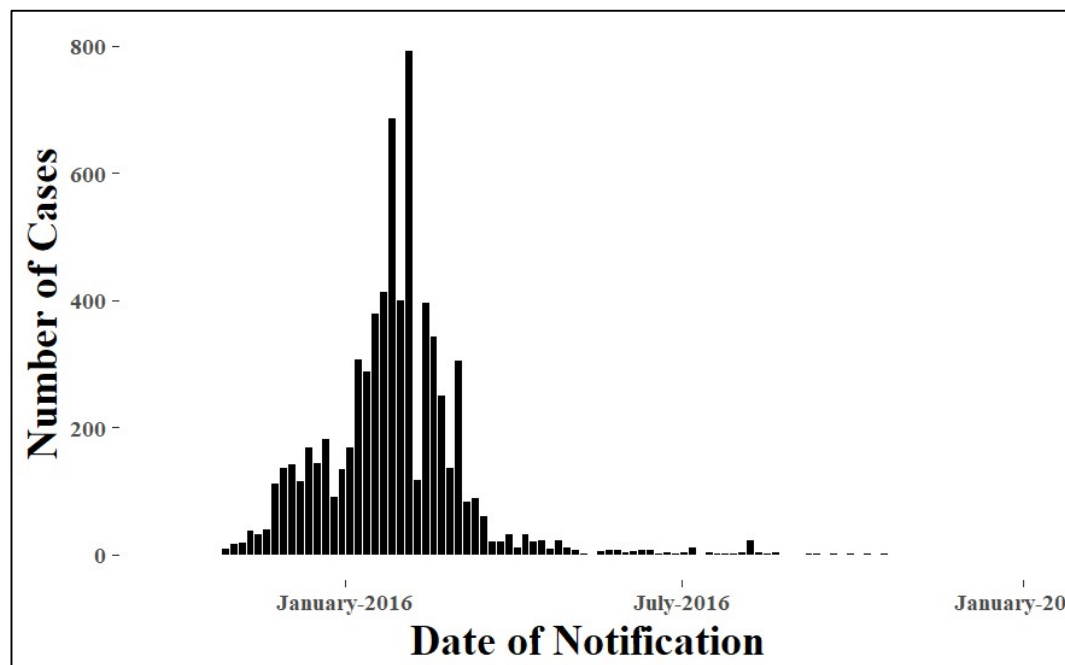

The map that displayed the total incidence rate by neighbourhood showed a small focus of high incidence in the south-western area of the city (Figure S5). The global univariate Moran's I statistic for the total incidence of ZIKV during the study period was 0.031 (pseudo p-value 0.191), thus there was not a clear global clustering pattern for this infection in Barranquilla. However, the LISA analysis showed three distinct small hotspots in the northern, south-western and south-eastern areas of the city (Figure S6).

The evolution of the ZIKV outbreak was less dramatic compared to that of the CHIKV epidemic, as revealed by the differential LISA analysis. However, a clear focus of hotspots occurred at the beginning of the outbreak in the north-western (neighbourhoods: 0307, 0308, 0311 and 0312) area of the city. These hotspots then evolved to the north-eastern area during November to December 2015 and then moved to the margins of the eastern side of the city (neighbourhoods: 2101, 2102 and 0804) located next to the main circular road around the city

14

and also neighbourhood 2102 located around the main city harbour during January to February 2016. As the outbreak waned during February to March, the hotspots returned to the north-eastern area of the city (Figure 6).

Figure 6. Differential monthly LISA clusters of ZIKV cases during the period of peak incidence (October 2015 – April 2016). Coloured neighbourhoods were significant, defined as p < 0.05. NS: not significant (grey colour).

15
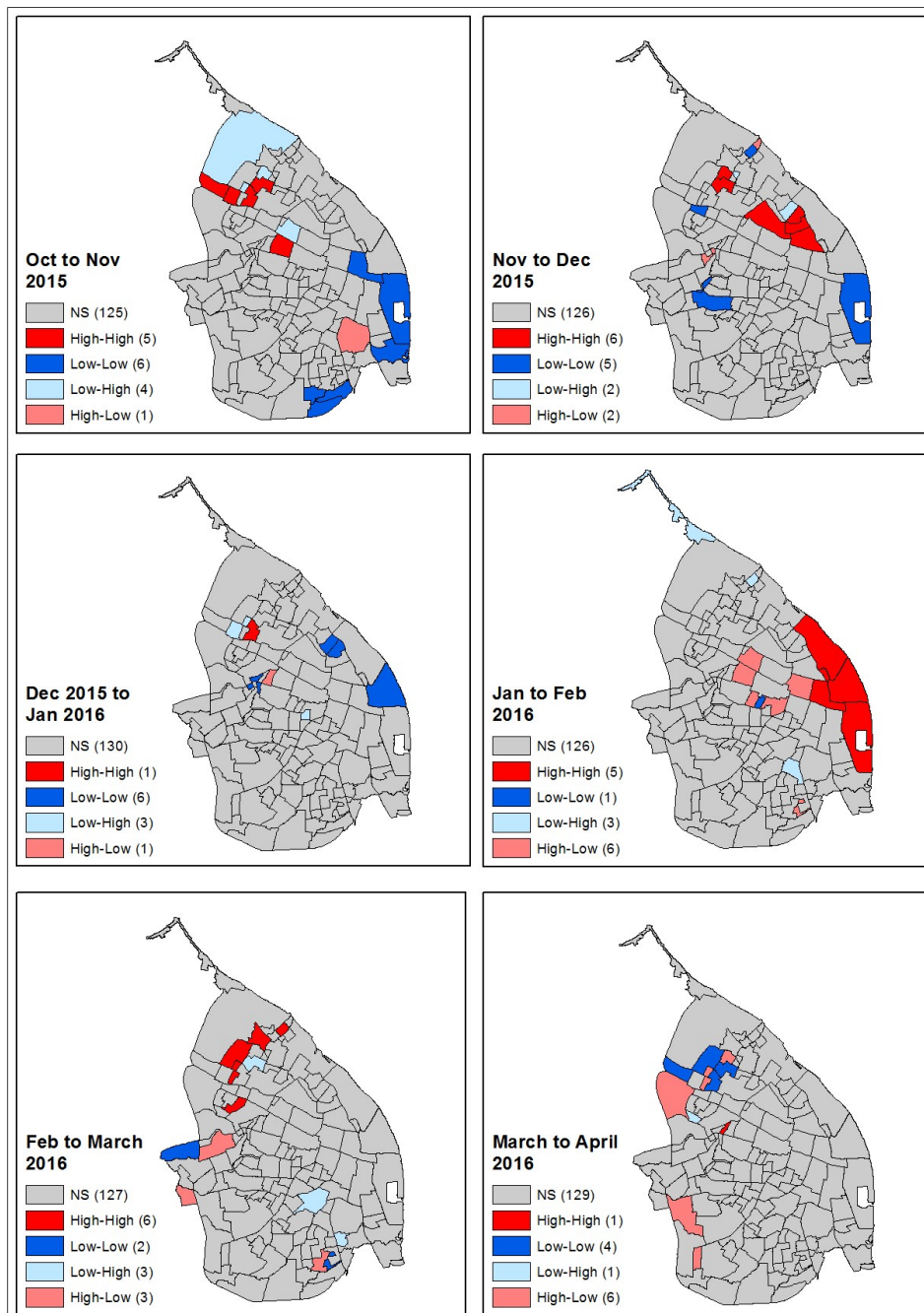
As with the CHIKV SIR, the Bayesian Poisson model of the ZIKV SIR fitted with the explanatory variables and with no random effects showed a poor fitting performance of incidence data (DIC: 2815.3) (Table 4). Thus, we introduced a set of independent random effects using the model 2 approach (Text S2) to capture the remaining variability. Unlike the CHIKV SIR model 2, we did not find any significant residual spatial correlation at a global scale (Moran's I statistic: 0.0101, p-value: 0.329) upon fitting the ZIKV SIR data based on the model 2 approach. However, a local Moran I statistic clearly showed the presence of some residual local spatial dependence (Figure S7). Therefore, we fitted a locally smooth CAR model with spatially correlated random effects (Text S2), which demonstrated better fitting performance comparing to previous modelling approaches (DIC: 957.6) (Table 4). Figure 7 shows crude and fitted ZIKV SIR values throughout Barranquilla.

Figure 7. Crude SIR of ZIKV infected cases by neighbourhood during its 2015-2016 epidemic in Barranquilla. (A) Fitted locally smooth CAR model for SIR with spatially correlated random effects and (B) the modelled SIR with spatially correlated random effects.
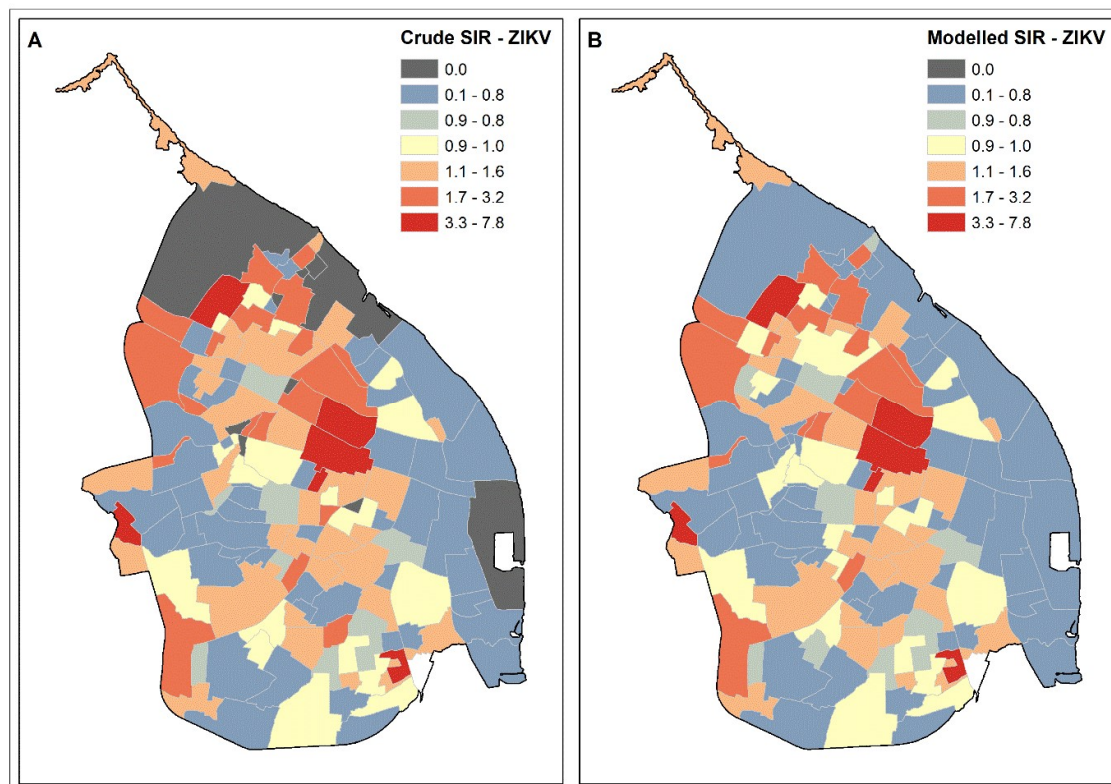
Table 3 displays the regression coefficients for the spatial fixed effects considered to fit the ZIKV SIR values based on the model 4 approach. The risk for ZIKV case incidence did not vary or varied very little according to the distance of dwellings from parks, water bodies, or the percentage of vegetation coverage. Surprisingly, the proportion of female residents also did not appear to be associated with the ZIKV infection risk. However, the richest neighbourhoods (SES 5 and 6) seemed to be significantly more at risk for ZIKV infections compared to those of the low and medium SES (p-value < 0.05) (Table 3 and Figure S8 SES map). In addition, the residents in the neighbourhoods with a higher percentage of dwellings that were houses (compared to apartments) had a higher risk for ZIKV infections (Coefficient 1.011, 95% CI 1.003, 1.020, p<0.05) (Table 3 and Figure S9 detached house map).

Table 3. Posterior median and 95% credible intervals for the fixed effects of the final model for the ZIKV standardized incidence rate (SIR) during 2014-2015. These parameters were reported on the exponential scale so that the effect could be interpreted as multiplicative on the SIR. Socioeconomic strata (SES) were grouped in three categories: high (SES 5 and 6), medium (SES 3 and 4) and low (SES 1 and 2), and regression coefficients were obtained for the medium SES and high SES compared to the low SES.

	Regression Coefficient	95% CI
Intercept	0.64	(0.49, 0.83)
Medium SES (ref. class low)	0.96	(0.68, 1.35)
High SES (ref. class low)*	3.02	(1.71, 5.40)
Population density	0.99	(0.98 1.01)
Housing density	0.98	(0.92, 1.40)
Percent house dwellings	1.01	(1.00, 1.02)
Percent female	1.06	(0.99, 1.12)
Percent vegetation coverage	1.00	(0.99, 1.01)
Distance from large water bodies	1.09	(0.89, 1.35)
Distance from parks	0.90	(0.65, 1.23)

*Significant association (p-value<0.05)

Table 4. DIC values for Bayesian Poisson Models

	CHIKV	ZIKV
Model 1: No random effects	1217.0421	2815.3024
Model 2: Independent random effects	718.2285	976.0006
Model 3: Globally smooth CAR	717.0342	-
Model 4: Locally smooth CAR	-	957.6401

DISCUSSION

The global cluster analysis of the CHIKV infected case incidences identified hotspots of transmission in the south-western area of the city. The monthly analysis of local autocorrelation showed that the CHIKV epidemic began within hotspots in the northern area and then moved quickly to the south-western region of this city, affecting mostly the poorest communities, following the main western circular route (circumvent roads) that also connects via a road with the principal truck transport depot and the south road to the city of Cartagena (Figures 1 and 3). The epidemic then appeared to spread back to the north of the city and to the south-east of the city via the main circular road. However, it may have also been re-introduced via boats arriving in the main sea dock area or via the road route (southeast direction) to the city of Santa Marta, and finally being transported from those northern neighbourhoods to the adjacent ones in December to January 2015. While there was little global spatial autocorrelation for the ZIKV infected case incidence, the monthly analysis of local autocorrelation showed a high-risk area in the northern neighbourhoods of the city as the outbreak began. As the outbreak intensified, the central-eastern neighbourhoods of the city became important hotspots. It seems that ZIKV epidemic spread to the eastern part of the city through the circumvent road following a clockwise direction probably via the cities major road routes (Figure 6 and Figure 1).

Using Bayesian Poisson regression allowing for random effects and controlling for all the covariates (fixed effects) in Tables 2 and 3, we found weak evidence that lower SES, decreasing percentage of vegetation coverage, and increasing distance from parks and large water bodies were associated with higher SIR of CHIKV infection. We found very strong evidence that higher SES had a higher risk for ZIKV infection and strong evidence that

18

increasing percent of house dwellings in a neighbourhood was associated with a higher risk for ZIKV infection.

We believe this is the first report that provides strong evidence that living in higher SES is a risk factor for ZIKV case incidences. Furthermore, the northern neighbourhoods of Barranquilla are of these higher SES and these neighbourhoods located there were the first to be infected and appeared to drive both the CHIKV and ZIKV outbreaks. Unfortunately, the local health authority's vector surveillance and control teams stated that it has been difficult to implement their work in areas of higher SES. Thus, limited, or lack of, access to identify and treat vector-breeding sites in these areas may have accounted for their higher ZIKV case incidence.

Alternatively, these findings may indicate a reporting bias resulting from these residents having better access to health facilities with resultant higher positive diagnosis rates. The issue of reporting bias was likely exacerbated during the ZIKV epidemic by the widespread media coverage drawn by the association of ZIKV with congenital defects. Those with easier access to clinics would have been more likely to present to clinic with milder symptoms and receive the diagnosis of ZIKV as it was sweeping through the city. In addition people living in higher socioeconomic strata would be more likely to be receiving regular prenatal healthcare, where there is already an over diagnosis of ZIKV [44]. Thus, the health authority team's access to these high-risk areas is urgently required to assess whether these results were due to the lack of vector surveillance and control or a higher incidence of case reporting. To our knowledge, higher incidences of vector-borne diseases have usually been associated with lower socioeconomic status [26,45,46,47] often due to poor sanitation and limited access to piped water leading to their need to store domestic water supplies in large water containers, which act as principal breeding sites for the *A. aegypti* vector species as reported in our study sites [48-50]. The two groups at most risk for DENV infections in Itaipu, Brazil were the lowest income population and a group in a slightly higher SES who had the funds to buy and store domestic water in large tanks [51]. The evidence we present here indicates that the CHIKV and ZIKV epidemics occurred in different ecological niches, with higher incidences of CHIKV infection in the poorer communities living on the periphery of the city.

Our Bayesian analysis, controlling for fixed effects revealed that neighbourhoods with greater distances from parks was associated with lower incidence of both CHIKV and ZIKV infections. This may indicate an increase in vector production in parks as areas of vegetation

19

that are more likely to collect pools of standing water. However, we were unable to show an association of either CHIKV or ZIKV infection with percent vegetation coverage. This may reflect a sensitivity in LandSat imaging that is unable to detect small vegetative surfaces such as parks. We also failed to show an association with population or housing density. These variables may not reflect the true numbers as they are based on projections from the 2005 census data [20]. We also found that neighbourhoods with a higher percent of female residents were at a higher risk for CHIKV and ZIKV infection. As discussed above, this may reflect an increased utilization of healthcare services by females

Through conversations with the vector control teams, the most common breeding site in apartments were flowerpots. While these were commonly positive for *Aedes aegypti* pupae, they do not produce large numbers of pupae and therefore resultant adult vectors [50,52]. Houses, on the other hand, are much more likely to have gardens or yards with or without patios that contain used or discarded water-holding containers, as well as very large domestic water storage containers (drums and tanks) which are the principal *Ae. aegypti* breeding sites, holding up to 92% of the pupae populations [52]. Previous studies have found that residents living in apartments were at a reduced risk for DENV infections [44,46,53], probably due to reduced availability of suitable sites for *Ae. aegypti* breeding [46,54]. Our data supported these findings since neighbourhoods with higher percentages of houses had significantly higher ZIKV case incidences and the south-western area of the city (which has higher percentages of detached houses) was an important hotspot in the CHIKV outbreak. Few studies have reported the incidences of CHIKV or ZIKV infected cases, but much lower combined *Aedes* spp. premise indexes—an indicator of premises with active breeding sites— were reported in apartments rather than compound houses in Singapore [39]. Surprisingly, however, *A. aegypti* was shown to have adapted to breeding in the 'ecosystems' present on each floor of high-rise apartment buildings in Kuala Lumpur, Malaysia [55].

Drawing spatial distinctions between the CHIKV and ZIKV cases assumed that the infected cases reported for these analyses were accurately identified. However, there are known limitations for accurate clinical discrimination amongst arboviral infections especially since financial restraints made it impossible to perform laboratory confirmation on all suspected cases. Previous projects in Barranquilla further evaluated the frequency with which these methods were used and found that only 1% of ZIKV and 1.7% of CHIKV infected cases were laboratory confirmed [24,25]. Since the CHIKV and ZIKV outbreaks occurred in separate

20

time periods, misclassification was more likely to have occurred only with the DENVs for which all 4 serotypes were previously shown to be endemic in Barranquilla [56,57]. While some studies have been limited by cross reactivity of IgM and IgG antibodies generated by patients with DENV and ZIKV (both flaviviruses) infections [58,59], all the laboratory-confirmed ZIKV cases in our study were identified by a positive ZIKV-specific RT-PCR.

We minimised the limitations of the modifiable area unit problem (MAUP) [60-62] in our study by using neighbourhoods as the unit of analysis, which was the smallest possible resolution available to us. However, while these analyses identified neighbourhood-level risk factors, the ecological fallacy prevented us from interpolating this to individual risk level. The statistical regression was limited by the possibility of residual confounding. There were several variables that we were unable to evaluate. The ethnicity of the people living in each neighbourhood may be important as shown in other studies, where Afro-Colombians were shown to have lower DENV infected case incidences [26,63]. Occupation, especially since it affects the movement of populations towards and away from neighbourhoods with various disease risk factors, may play an important role, as was reported for DENV infected case incidences in poor neighbourhoods with high populations of young (<15 year old) [44,64], illiterate and unemployed people in Cali, Colombia [65]. Housing data was unavailable for 30% of the neighbourhoods, while the percentage of dwellings that were houses or apartments was unavailable for 19% of the neighbourhoods. We used a multiple imputation approach to mitigate the effect of unavailable data. This assumed that the unavailable data was missing at random and the imputation model is correctly specified [66].

The findings in our study are novel in their attempt to correlate previous epidemiological patterns of DENV infected case incidence neighbourhood risk factors discussed above with those of recent outbreaks of CHIKV and ZIKV. Our spatial exploration clearly identified neighbourhoods that had been hotspots responsible for driving the epidemic waves of CHIKV and ZIKV. It is therefore essential that these hotspots are constantly targeted by the local Health Authorities to reduce *A. aegypti* breeding sites to a minimum and quickly act to target all areas in and surrounding them when any cases of CHIV or ZIKV are reported. The risk factor analysis provided strong evidence that higher socioeconomic status was a risk factor for ZIKV. In Barranquilla, the Public Health Department should be empowered to commit more resources to these areas of the city. While it may seem counterintuitive to direct public resources to areas of higher SES, determining whether higher *Ae. aegypti* vector populations

or increased residents' reporting urgently needs to be assessed. If the former case was responsible, then the public health authorities must identify and destroy the vector breeding sites through drainage or larvacidal treatment.

Finally, further research needs to be performed to account for differences in vector, invasion, breeding and disease transmission. More in-depth data about housing vulnerability could include type of building material, exposure to the outside, and presence of air conditioning, since home air conditioning was a major factor accounting for the much lower DENV sero-positivity for the residents in a study site in Texas, USA compared to that in a twined town in Mexico [67]. Collecting this information could reduce the residual bias associated with our crude measure of housing type. Further analysis should assess these arboviral case incidences with the residents' occupation and other forms of population movement. More detailed vector surveillance is also needed throughout the city to elucidate why the risk factors identified in this study are associated with higher transmission. Since no effective treatments or vaccines exist for CHIKV and ZIKV, prevention is still the primary method of control [8,9,68].

CONCLUSIONS

This study provided an evidence-based framework that public health programmes can use to efficiently target the drivers of future epidemics of CHIKV and ZIKV infections. Our spatial analysis identified key areas of Barranquilla that acted as hotspots during the outbreaks of CHIKV and ZIKV. Furthermore, we clearly showed that living in the high SES was a risk factor for ZIKV transmission and these richer areas were important hotpots of case incidence during both outbreaks. This novel finding challenges the logic that *Ae. aegypti*-borne infections are driven by social vulnerability and merits further study both in Barranquilla and throughout the tropical and sub-tropical areas of the world.

22

Supplementary Materials

Table S1. Neighbourhood names with their corresponding codes, as used in the Barranquilla map (Figure 1).

Figure S1: Satellite image from Landsat 8 mission for the Barranquilla area obtained in December 2014. The image shows maps of natural band combination (4-3-2) and infrared colour combination (5-4-3), and the derived products that resulted from the supervised classification and calculation of the MNDWI.

Figure S2. Satellite image from Landsat 8 mission for the Barranquilla area obtained in December 2015. The image shows maps of natural band combination (4-3-2) and infrared colour combination (5-4-3), and the derived products that resulted from the supervised classification and calculation of MNDWI.

Figure S3. The estimated incidence of CHIKV infected cases per 10,000 residents by neighbourhood in Barranquilla between 2014 and 2015.

Figure S4. The univariate Local Moran's I (LISA) cluster map of the overall incidence of CHIKV infected cases during 2014-2016.

Figure S5. The estimated incidence of ZIKV infected cases per 10,000 residents by neighbourhood in Barranquilla between 2015 and 2016.

Figure S6. The univariate Local Moran's I (LISA) cluster map of the overall incidence of ZIKV infected cases during 2014-2016.

Figure S7. Local Moran's I analysis on the residuals resulting from fitting the ZIKV SIR values with spatial explanatory variables and independent random effects. Maps show (A) the persisting local clusters and (B) their corresponding p-values.

Figure S8. Socioeconomic strata (SES) designation for each neighbourhood in Barranquilla.

Figure S9. Percentage of dwellings that were detached houses in each neighbourhood in Barranquilla.

Text S1. Implementation of spatial autocorrelation analysis (Global Moran's I statistic & Local Indicator of Spatial Autocorrelation, LISA).

Text S2. Details on the implementation of Bayesian statistical modelling.

Abbreviations

CAR: conditional autoregressive models; DENV: dengue virus; CHIKV: chikungunya virus; DIC: deviance information criterion; LISA: local indicator of spatial autocorrelation; MNDWI: modification of the normalised difference water index; SIR: standardized incidence rate; ZIKV: Zika virus

Authors' contribution

Conceptualization and methodology, TM, JC and CR; software, TM, JC and CF; validation, TM, JC, CR, CF and AF; formal analysis, TM, JC and CF; investigation, TM; resources, CR, AF, PA, NW and CN; data curation, TM, JC, CF and PA; writing—original draft preparation, TM; writing—review and editing, TM, JC, CR, AF, NW and CN; visualization, TM and JC; supervision, JC, CR and AF; project administration, JC, CR and AF; funding acquisition, JC, CR and AF. All authors have read and approved of the manuscript.

Conflicts of Interest

The authors declare no conflict of interest.

Acknowledgements

Funding

REFERENCES

1. Cassadou S.; Boucau S.; Petit-Sinturel M.; Huc P.; Leparc-Goffart I.; Ledrans M. Emergence of chikungunya fever on the French side of Saint Martin island, October to December 2013. *Euro Surveill.* **2014**, 19, 20752.

2. Fernández-Salas I.; Danis-Lozano R.; Casas-Martínez M.; Ulloa A.; Bond J.G.; Marina C.F.; Lopez-Ordoñez T.; Elizondo-Quiroga A.; Torres-Monzón J.A.; Diaz-González E.E. Historical inability to control Aedes aegypti as a main contributor of fast dispersal of chikungunya outbreaks in Latin America. *Antiviral Res.* **2015**, 124, 30-42.

3. Halstead S.B. Reappearance of chikungunya, formerly called dengue, in the Americas. *Emerg. Infect. Dis.* **2015**, 21, 557.

4. Zanluca C.; Melo, V.C.; Mosimann A.L.; Santos G.I.; Santos C.N.; Luz K. First report of autochthonous transmission of Zika virus in Brazil. *Mem. Inst. Oswaldo Cruz* **2015**, 110, 569-572.

5. Alvis-Guzman N.; Zakzuk-Sierra J.; Vargas-Moranth R.; Alcocer-Olaciregui A.; Parra-Padilla D. Dengue, Chikunguna y Zika en Colombia 2015-2016. *Revista MVZ Cordoba* **2017**, 22(suppl), 5994-6003.

6. Cardona-Ospina J.A.; Villamil-Gomez W.E.; Jimenez-Canizales C.E.; Castañeda-Hernåndez D.M.; Rodriguez-Morales A.J. Estimating the burden of disease and the economic cost attributable to chikungunya, Colombia, 2014. *Trans. R. Soc. Trop. Med. Hyg.* **2015**, 109, 793-802.

7. Cuevas E.L. Preliminary report of microcephaly potentially associated with Zika virus infection during pregnancy—Colombia, January–November 2016. *Morb. Mortal. Wkly. Rep.* **2016**, 65, 1409-1413.

8. Staples J.E.; Fischer M. Chikungunya virus in the Americas—what a vectorborne pathogen can do. *N. Engl. J. Med.* **2014**, 371, 887-889.

9. Petersen L.R.; Jamieson D.J.; Powers A.M.; Honein M.A. Zika virus. *N. Engl. J. Med.* **2016**, 374, 1552-1563.

10. Rasmussen S.A.; Jamieson D.J.; Honein M.A.; Petersen L.R. Zika virus and birth defects—reviewing the evidence for causality. *N. Engl. J. Med.* **2016**, 374, 1981-1987.

11. Musso D.; Gubler D.J. Zika virus. *Clin. Microbiol. Rev.* **2016**, 29, 487-524.

12. Stewart-Ibarra A.M.; Lowe R. Climate and non-climate drivers of dengue epidemics in southern coastal Ecuador. *Am. J. Trop. Med. Hyg.* **2013**, 88, 971-981.

13. Wilder-Smith A, Gubler DJ. Geographic expansion of dengue: the impact of international travel. Med Clin North Am 2008;92(6):1377-1390.

14. Khormi H.M.; Kumar L. Modeling dengue fever risk based on socioeconomic parameters, nationality and age groups: GIS and remote sensing based case study. *Sci. Total Environ.* **2011**, 409, 4713-4719.

15. Sissoko D.; Moendandze A.; Malvy D.; Giry C.; Ezzedine K.; Solet J.L.; Pierre V. Seroprevalence and risk factors of chikungunya virus infection in Mayotte, Indian Ocean, 2005-2006: a population-based survey. PloS one 2008;3(8):e3066.

16. Perkins T.A.; Metcalf C.J.E.; Grenfell B.T.; Tatem AJ. Estimating drivers of autochthonous transmission of chikungunya virus in its invasion of the Americas. *PLoS Curr.* **2015**, 7, ecurrents.outbreaks.a4c7b6ac10e0420b1788c9767946d1fc.

17. Bogoch I.I.; Brady O.J.; Kraemer M.U.; German M.; Creatore M.I.; Kulkarni M.A.; Brownstein J.S.; Mekaru S.R.; Hay S.I.; Groot E. et al. Anticipating the international spread of Zika virus from Brazil. *The Lancet* **2016**, 387, 335-336.

18. Samy A.M.; Thomas S.M.; Wahed A.A.E.; Cohoon K.P.; Peterson A.T. Mapping the global geographic potential of Zika virus spread. *Mem. Inst. Oswaldo Cruz* **2016**, 111, 559-560.

19. Paz S.; Semenza J.C. El Niño and climate change—contributing factors in the dispersal of Zika virus in the Americas? *The Lancet* **2016**, 387, 745.

20. Estadistica, Departamento Administrativo Nacional de. DANE. 2017; Available at: http://www.dane.gov.co. Accessed 02, 2017.

21. Orozco A. El sector salud en las ciudades colombianas de Barranquilla y Cartagena. Lecturas de Economía 2014, 80, http://aprendeenlinea.udea.edu.co/revistas/index.php/lecturasdeeconomia/article/view/18542

22. Perkins TA, Siraj AS, Ruktanonchai CW, Kraemer MU, Tatem AJ. Model-based projections of Zika virus infections in childbearing women in the Americas. *Nature Microbiol.* **2016**, 1, 16126.

23. Tarantine C. Dengue Fever Surveillance System in Barranquilla, Colombia. MSc Control of Infectious Disease, University of London, The London School of Hygiene and Tropical Medicine, August 2013.

24. Walker N. Investigation of the Chikungunya Virus Outbreak in Barranquilla, Colombia, and Evaluation of the Surveillance System for Chikungunya in Place During the Outbreak. MSc Control of Infectious Disease, University of London, The London School of Hygiene and Tropical Medicine, August 2014.

25. Nix C. Investigation into the transmission of Zika virus in Barranquilla, Colombia. MSc Control of Infectious Disease, University of London, The London School of Hygiene and Tropical Medicine, August 2015.

26. Delmelle E.; Hagenlocher M.; Kienberger S.; Casas I. A spatial model of socioeconomic and environmental determinants of dengue fever in Cali, Colombia. *Acta. Trop.* **2016**, 164, 169-176.

27. Botero D.S.; Bocanegra D. Protocolo de vigilancia en salud publica. Chikungunya. Instituto Nacional de Salud. **2016**, 1-33. http://www.cruevalle.org/files/PRO-Chikungunya.pdf

28. Tolosa Pérez N.; Ospina Martinez M.L.; Martinez Duran M.E.; Pacheco Garcia O.E.; Quijada B.H. Protocolo de Vigilancia en Salud Pública: Enfermedad por Virus Zika. Instituto Nacional de Salud. **2016**, 1-27. http://bvs.minsa.gob.pe/local/MINSA/3449.pdf

29. Llerena K.A. Portal Democrativa Participación & nbsp; 2017; Available at: http://participacion.barranquilla.gov.co. Accessed 01.08.2017.

30. Explorer U.E. EarthExplorer. Available from Internet: http://edcsns17.cr.usgs.gov/NewEarthExplorer 2017;122.

31. Zhang Z.; He G.; Wang X. A practical DOS model-based atmospheric correction algorithm. *Int. J. Remote Sens.* **2010**, 31, 2837-2852.

32. Xu D.; Guo X. Compare NDVI extracted from Landsat 8 imagery with that from Landsat 7 imagery. *Am. J. Remote Sens.* **2014**, 2, 10-14.

33. Ukolova O. OpenWeatherMap. 2017; Available at: https://openweathermap.org. Accessed 1.8.2017.

34. Han-Qiu X.U. A Study on Information Extraction of Water Body with the Modified Normalized Difference Water Index (MNDWI)[J]. *J. Remote Sens.* **2005**, 5, 589-595.

35. ESRI. ArcGIS Desktop: Release 10. 2017;10.3.

36. Sainte-Marie M. The Road to Direction: An Agent-Based Simulation of Human Movement using Directed Street Topologies. Spatial Cognition IX: International Conference, Spatial Cognition 2014, Bremen, Germany, September 15-19, **2014**, Editors: Christian Freksa, Bernhard Nebel, Mary Hegarty, Thomas Barkowsky, Lecture Edition, Springer, pp 206-221.

37. Anselin L. Exploring Spatial Data With GeoDa: A Work Book. Spatial Analysis Laboratory, University of Illinois. Center for Spatially Integrated Social Science 2005. http://www.csiss.org/clearinghouse/GeoDa/geodaworkbook.pdf

38. Anselin L.; Syabri I.; Kho Y. GeoDa : An Introduction to Spatial Data Analysis. *Geogr. Anal.* **2006**, 38, 5-22.

39. Anselin L. Local indicators of spatial association—LISA. *Geogr. Anal.* **1995**, 27, 93-115.

40. Anselin L. Under the hood Issues in the specification and interpretation of spatial regression models. *J. Agric. Econ.* **2002**, 27, 247-267.

41. Besag J.; York J.; Mollie A. Bayesian image restoration, with two applications in spatial statistics. *Ann. Inst. Statist. Math.* **1991**, 43, 1-20.

42. Lee D.; Mitchell R. Locally adaptive spatial smoothing using conditional auto-regressive models. *J. R. Stat. Soc. Series C (Appl. Stats.)* **2013**, 62, 593-608.

43. Spiegelhalter D.J.; Best N.G.; Carlin B.P.; Van Der Linde A. Bayesian measures of model complexity and fit. *J. R. Stat. Soc. Series B (Stat. Meth.)* **2002**, 64, 583-639.

44. Pacheco O.; Beltrán M.; Nelson C.A.; Valencia D.; Tolosa N.; Farr S.L.; Padilla A.V.; Tong V.T.; Cuevas E.L.; Espinosa-Bode A. et al. Zika virus disease in Colombia—preliminary report. *N. Engl. J. Med.* 2016, DOI: 10.1056/NEJMoa1604037

45. Braga C.; Luna C.F.; Martelli C.M.; De Souza W.V.; Cordeiro M.T.; Alexander N.; de Albuquerque Mde F.; Júnior J.C.; Marques E.T. Seroprevalence and risk factors for dengue infection in socio-economically distinct areas of Recife, Brazil. *Acta. Trop.* **2010**, 113, 234-240.

46. Koh B.K.; Ng L.C.; Kita Y.; Tang C.S.; Ang L.W.; Wong K.Y.; James L.; Goh K.T. The 2005 dengue epidemic in Singapore: epidemiology, prevention and control. Ann. Acad. Med. Singapore 2008, 37, 538-545.

47. Mondini A.; Chiaravalloti-Neto F. Spatial correlation of incidence of dengue with socioeconomic, demographic and environmental variables in a Brazilian city. *Sci. Total Environ.* **2008**, 393, 241-248.

48. Romero-Vivas C.M.; Llinás H; Falconar A.K. Three calibration factors, applied to a rapid sweeping method, can accurately estimate Aedes aegypti (Diptera: Culicidae) pupal numbers in large water-storage containers at all temperatures at which dengue virus transmission occurs. *J. Med. Entomol.* **2007**, 44, 930-937.

49. Romero-Vivas C.M.; Falconar AK. Investigation of relationships between Aedes aegypti egg, larvae, pupae, and adult density indices where their main breeding sites were located indoors. *J. Am. Mosq. Control Assoc.* **2005**, 21, 15-21.

50. Romero-Vivas C.M.; Arango-Padilla P.; Falconar A.K. Pupal-productivity surveys to identify the key container habitats of Aedes aegypti (L.) in Barranquilla, the principal seaport of Colombia. *Ann. Trop. Med. Parasitol.* **2006**, 100(supp 1), 87-95.

51. San Pedro A.; Souza-Santos R.; Sabroza P.C.; Oliveira RMd. Condições particulares de produção e reprodução da dengue em nível local: estudo de Itaipu, Região Oceânica de Niterói, Rio de Janeiro, Brasil. *Cadernos de Saúde Pública* **2009**, 25, 1937-1946.

52. Romero-Vivas C.M.; Wheeler J.G.; Falconar A.K. An inexpensive intervention for the control of larval Aedes aegypti assessed by an improved method of surveillance and analysis. *J. Am. Mosq. Control Assoc.* **2002**, 18, 40-46.

53. Zellweger R.M.; Cano J.; Mangeas M.; Taglioni F.; Mercier A.; Despinoy M.; Menkès C.E.; Dupont-Rouzeyrol M.; Nikolay B.; Teurlai M. Socioeconomic and environmental determinants of dengue transmission in an urban setting: An ecological study in Nouméa, New Caledonia. *PLoS Negl. Trop. Dis.* **2017**, 11, e0005471.

54. Carbajo A.E.; Curto S.I.; Schweigmann N.J. Spatial distribution pattern of oviposition in the mosquito Aedes aegypti in relation to urbanization in Buenos Aires: southern fringe bionomics of an introduced vector. *Med. Vet. Entomol.* **2006**, 20, 209-218.

55. Roslan M.A.; Shafie A.; Ngui R.; Lim Y.A.L.; Sulaiman W.Y.W. Vertical infestation of the dengue vectors Aedes aegypti and Aedes albopictus in apartments in Kuala Lumpur, Malaysia. *J. Am. Mosq. Control Assoc.* **2013**, 29, 328-336.

56. Falconar A.K.; de Plata E.; Romero-Vivas C.M. Altered enzyme-linked immunosorbent assay immunoglobulin M (IgM)/IgG optical density ratios can correctly classify all primary or secondary dengue virus infections 1 day after the onset of symptoms, when all of the viruses can be isolated. *Clin. Vaccine Immunol.* **2006**, 13, 1044-1051.

57. Falconar A.K.; Romero-Vivas C.M. Simple prognostic criteria can definitively identify patients who develop severe versus non-severe dengue disease, or have other febrile illnesses. *J. Clin. Med. Res.* **2012**, 4, 33.

58. Duffy M.R.; Chen T.; Hancock W.T.; Powers A.M.; Kool J.L.; Lanciotti R.S.; Pretrick M.; Marfel M., Holzbauer S., Dubray C. et al. Zika virus outbreak on Yap Island, federated states of Micronesia. *N. Engl. J. Med.* **2009**, 360, 2536-2543.

59. Waggoner J.J.; Pinsky B.A. Zika virus: diagnostics for an emerging pandemic threat. *J. Clin. Microbiol.* **2016**, 54, 860-867.

60. Flowerdew R.; Manley D.J; Sabel CE. Neighbourhood effects on health: does it matter where you draw the boundaries? *Soc. Sci. Med.* **2008**, 66, 1241-1255.

61. Jelinski D.E.; Wu J. The modifiable areal unit problem and implications for landscape ecology. *Landscape Ecol.* **1996**, 11, 129-140.

62. Stafford M.; Duke-Williams O.; Shelton N. Small area inequalities in health: are we underestimating them? *Soc. Sci. Med.* **2008**, 67, 891-899.

63. Rojas Palacios J.H.; Alzate A.; Martínez Romero H.J.; Concha-Eastman A.I. AfroColombian ethnicity, a paradoxical protective factor against Dengue. *Colomb. Med. (Cali)* **2016**, 47, 133-141.

64. Yew Y.W.; Ye T.; Ang L.W.; Ng L.C.; Yap G.; James L.; Chew S.K.; Goh K.T. Seroepidemiology of dengue virus infection among adults in Singapore. Ann. Acad. Med. Singap. **2009**, 38, 667-675.

65. Hagenlocher M.; Delmelle E.; Casas I.; Kienberger S. Assessing socioeconomic vulnerability to dengue fever in Cali, Colombia: statistical vs expert-based modeling. *Int. J. Health. Geogr.* **2013**, 12, 36.

66. Sterne J.A.; White I.R.; Carlin J.B.; Spratt M.; Royston P.; Kenward M.G.; Wood A.M.; Carpenter J.R. Multiple imputation for missing data in epidemiological and clinical research: potential and pitfalls. *BMJ* **2009**, 338, b2393.

67. Reiter P.; Lathrop S.; Bunning M.; Biggerstaff B.; Singer D.; Tiwari T.; Baber L.; Amador M.; Thirion J.; Hayes J.; et al. Texas lifestyle limits transmission of dengue virus. *Emerg. Infect. Dis.* **2003**, 9, 86.

68. Webber R. *Communicable disease epidemiology and control: a global perspective.* 3rd ed. CABI, Wallingford, Oxfordshire, UK, 2009.